Journal of Fluorine Chemistry 183 (2016) 1–9

Contents lists available at ScienceDirect

Journal of Fluorine Chemistry

journal homepage: www.elsevier.com/locate/fluor

Thermal, structural, optical, dielectric and barocaloric properties at ferroelastic phase transition in trigonal $(NH_4)_2SnF_6$: A new look at the old compound

Igor N. Flerov[a,b,*], Andrey V. Kartashev[a,c], Mikhail V. Gorev[a,b], Evgeniy V. Bogdanov[a,d], Svetlana V. Mel'nikova[a], Maxim S. Molokeev[a,e], Evgeniy I. Pogoreltsev[a,b], Natalia M. Laptash[f]

[a] Kirensky Institute of Physics, Siberian Branch of RAS, 660036 Krasnoyarsk, Russia
[b] Institute of Engineering Physics and Radioelectronics, Siberian State University, 660074 Krasnoyarsk, Russia
[c] Astafijev Krasnoyarsk State Pedagogical University, 660049 Krasnoyarsk, Russia
[d] Krasnoyarsk State Agrarian University, 660049 Krasnoyarsk, Russia
[e] Far Eastern State Transport University, 680021 Khabarovsk, Russia
[f] Institute of Chemistry, Far Eastern Branch of RAS, 690022 Vladivostok, Russia

ARTICLE INFO

Article history:
Received 3 November 2015
Received in revised form 21 December 2015
Accepted 27 December 2015
Available online 3 January 2016

Keywords:
Fluorides
Structural disorder
Phase transitions
Entropy
Barocaloric effect

ABSTRACT

Structural phase transition P-3m1 ↔ P-1 of the first order and nonferroelectric nature was found in $(NH_4)_2SnF_6$ at about 110 K in the process of thermal, optical, dielectric and X-ray studies.

Order-disorder transformation is accompanied by large changes of entropy ($\Delta S_0 = 16.4$ J/mol K) and volume ($\Delta V_0/V \approx 1\%$). The structural model associated with three orientations of NH_4 tetrahedra in P-3m1 phase and their complete ordering in P-1 phase was suggested with the entropy change ($\Delta S_0 = 18.3$ J/mol K) close to the experimental value. A good agreement between baric coefficients measured in a direct way ($dT_0/dp = -157$ K/GPa) and evaluated using entropy and volume changes at phase transition (−170 K/GPa) was found. Barocaloric effects in $(NH_4)_2SnF_6$ are comparable with those of known solid state refrigerants and are characterised by a low-pressure need for realising their maximum values.

1. Introduction

Recent pioneering observations of phase transitions in fluoride double salts $(NH_4)_3TiF_7$ and $(NH_4)_3SnF_7$ have shown that these structural transformations were accompanied by the decomposition process at high temperatures, followed by the emergence of the $(NH_4)_2TiF_6$ and $(NH_4)_2SnF_6$ phases, which were used as the initial substances for the synthesis of both heptafluorocompounds [1,2]. The symmetry of both hexafluorocompounds was trigonal with the P-3m1 space group, $Z = 1$. In $(NH_4)_3TiF_7$, the decomposition process started at temperature rather far from phase transition points and did not prevent the study of physical properties, in particular, thermal properties [3]. X-ray powder studies of ammonium heptafluorostannate showed that the temperatures of both the direct phase transition between two cubic phases and the decomposition process were rather close to each other [2]. This circumstance could complicate the investigation of the physical properties behaviour at structural transformation especially integral thermodynamic characteristics such as enthalpy and entropy. Thus, before the studying thermal properties of $(NH_4)_3SnF_7$ in details we needed to know the same properties of $(NH_4)_2SnF_6$.

It was surprising that, despite the fact that ammonium hexafluorostannate has been known for many years [4], we have found scant information concerning this compound. The room temperature structure (sp. gr. P-3m1, $Z = 1$) containing isolated $[SnF_6]^{2-}$ octahedra and $[NH]^{4+}$ tetrahedra was first determined by X-ray powder diffraction [5] and then refined by the single crystal experiment [6]. It was also found that $(NH_4)_2SnF_6$, like other A_2SnF_6 compounds (A: K, Rb, Cs, Tl), can be obtained either in trigonal or cubic (sp. gr. Fm-3m, $Z = 4$) modification depending on the conditions of crystallisation [7]. In DTA-measurements only one reversible peak meaning the P-3m1 → Fm-3m transition was found in the range 450–520 °C for different alkaline hexafluorostannates.

* Corresponding author at: Kirensky Institute of Physics, Akademgorodok 50, bld.38, Krasnoyarsk 660036, Russia.
E-mail address: flerov@iph.krasn.ru (I.N. Flerov).

http://dx.doi.org/10.1016/j.jfluchem.2015.12.010
0022-1139/

Table 1
Main parameters of processing and refinement of the $(NH_4)_2SnF_6$ sample.

Compound	$(NH_4)_2SnF_6$
Sp.Gr.	P-3m1
a, Å	6.0711(2)
c, Å	4.8542(2)
V, Å^3	154.95(1)
Z	1
2θ-interval, °	5–120
No. of reflections	104
No. of refined parameters	29
R_{wp},%	8.15
R_p,%	5.98
R_{exp},%	5.33
χ^2	1.53
R_B,%	1.22

The same polymorphism was observed in the related compound $(NH_4)_2SiF_6$ [8,9].

Calorimetric experiments have revealed that the trigonal P-3m1 modification underwent order-disorder phase transition at about 38.6 K, whereas cubic modification remained stable at least down to 25 K, which was the lowest temperature of measurements [10]. Because the standard entropy found for P-3m1 phase ($S^\circ = 280.4 \pm 0.6$ J/mol K) was less than that for Fm-3 m phase ($S^\circ = 285.6 \pm 0.6$ J/mol K), trigonal modification can be considered as metastable. One can suppose that this is the reason of the conversion from trigonal phase to cubic observed at room temperature over time [10]. There is no information about the symmetry of phase realized below 38.6 K for trigonal $(NH_4)_2SiF_6$. Also, the mechanism of structural distortions has not been established. Order–disorder reorientations were attributed to either the SiF_6^{2-} anion [10] or the ammonium cation [11].

The study of optical and structural properties of $(NH_4)_3TiF_7$ and $(NH_4)_3SnF_7$ has shown that the increase of the central atom size Ti → Sn led to strong increase of the temperature of the phase transition from the low temperature cubic phase P-3a [1,2]. Taking into account the stronger difference between the Si and Sn ionic sizes one can suppose that a reversible structural phase transition observed in $(NH_4)_2SiF_6$ [10] could exist in trigonal $(NH_4)_2SnF_6$ at much higher temperatures compared to ammonium hexafluorosilicate.

In this paper, we present the results of structural, polarizing-optic and differential scanning calorimetric searching for phase transition in trigonal $(NH_4)_2SnF_6$ as well as detailed data on heat capacity, thermal dilatation and dielectric properties in a wide temperature range. Hydrostatic pressure effect as well as barocaloric efficiency were also investigated.

2. Sample preparation and characterization

Ammonium hexafluorostannate, $(NH_4)_2SnF_6$, was synthesised using metallic tin platelets (β-Sn) of the 99.9% purity as a starting material. Such a synthesis has been previously described [5], where the starting reagent was freshly precipitated meta-tin acid. We used chemically pure nitric acid (56 mass.% HNO_3) and hydrofluoric acid (40% HF) for tin oxidation and complexation in accordance with the reaction:

$$Sn + 6HF + 4HNO_3 = H_2SnF_6 + 4NO_2 + 4H_2O$$

Chemical etching tin platelets was carried out in the excess of HF with accurate dropwise addition of HNO_3 at room temperature because of high exothermal character of the above reaction. Ammonia aqueous solution (NH_3 aq, 25%) was then added to increase the solution pH from 0 to 2:

$$H_2SnF_6 + 2NH_3 = (NH_4)_2SnF_6$$

Thin hexagonal plates of $(NH_4)_2SnF_6$ were formed in the course of evaporation (the PXRD pattern were matching with the JCPDS file No. 026-0094)

The powder diffraction data of $(NH_4)_2SnF_6$ for Rietveld analysis were collected at room temperature with a Bruker D8 ADVANCE powder diffractometer (Cu-K radiation) and linear VANTEC detector. The step size of 2θ was 0.016°, and the counting time was 0.6 s per step. Rietveld refinement was performed using TOPAS 4.2 [12]. All peaks were indexed by the trigonal unit cell (P-3m1) with parameters close to those determined from single crystal experiments [6]. Therefore this crystal structure was chosen as the starting model for Rietveld refinement. Hydrogen atoms were omitted in the model considered. Refinement was stable and gave low R-factors (Table 1,Fig. 1).

Atomic coordinates presented in Table 2 are also in a good agreement with the single crystal data [6].

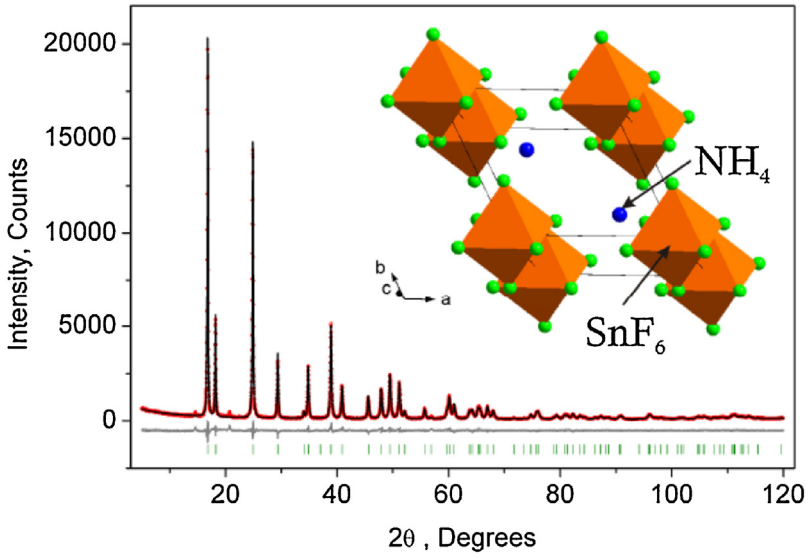

Fig. 1. Difference Rietveld plot of $(NH_4)_2SnF_6$. Inset shows the crystal structure.

Table 2
Fractional atomic coordinates and isotropic displacement parameters (Å^2) of $(NH_4)_2SnF_6$.

	x	*y*	*z*	B_{iso}
Sn	0	0	0	1.53 (6)
F	0.1553 (2)	0.3105 (5)	0.2132 (5)	2.52 (8)
N	2/3	1/3	0.309 (1)	2.2 (2)

3. Results and discussion

3.1. Searching for phase transition

By analogy with trigonal $(NH_4)_2SiF_6$ undergoing reversible phase transition at rather low temperatures [10], the probable decrease of the symmetry would be expected to exist upon cooling in $(NH_4)_2SnF_6$ too. In order to examine this hypothesis, calorimetric and optical studies of trigonal hexafluorostannate were performed in a wide temperature range 90–300 K.

A DSM–10 M differential scanning microcalorimeter (DSM) was used for the preliminary heat capacity $C_p(T)$ measurements. The powdered compound under study was placed into an aluminum sample holder. Temperature and enthalpy were calibrated using the melting parameters of pure indium. The temperatures were determined with an accuracy of ±1 K and the uncertainty on the enthalpy value was estimated as ±5 J/mol. The experiments were carried out in a He gaseous atmosphere on several samples from the same crystallization. The mass of the samples was ~0.06–0.10 g. Upon heating, at a rate of 8 K/min, a reversible anomalous behaviour of $C_p(T)$ was observed at $T_0 = 110 \pm 1$ K. We were not able to examine the T_0 hysteresis phenomenon because the lowest temperature in DSM experiments upon cooling was about 120 K.

Fig. 2a depicts the temperature dependence of the excess heat capacity ΔC_p evaluated as a difference between the total heat capacity C_p and nonanomalous lattice contribution C_{lat}.

The enthalpy change in $(NH_4)_2SnF_6$ associated with anomalous behaviour of C_p in the range 100–115 K was found as $\Delta H_0 = \int \Delta C_p dT = 1170 \pm 140$ J/mol (Fig. 2b).

In order to make sure that the heat phenomenon observed is associated with structural phase transition, we explored further the trigonal phase stability using polarizing microscope Axioskop-40 with a temperature chamber Linkam LTS 350.

At room temperature, hexagonal plates of $(NH_4)_2SnF_6$ were optically isotropic with the exit of the optical axis (0 0 1) (Fig. 3a). Upon cooling below T_0, a sharp front of the optical anisotropy appeared, accompanied by the formation of twinned structure as thin strips of different directions (Fig. 3b and c)

In the low temperature phase, the crystal has the extinctions in some separate parts (Fig. 3d). The situation is slightly different to the direct extinction. This is evident by an asymmetrically placed hexagon inside the frame of the picture. Six types of twin boundaries are seen in Fig. 3c and d as well as with a high magnification in Fig. 3f. Both experimentally observed facts allow us to assume that the phase transition in $(NH_4)_2SnF_6$ is accompanied by the loss of all axes and mirror planes existing in the P-3m1 phase. Thus, the symmetry of the low-temperature phase can be most likely characterised as triclinic with either the P-1 or P1 space group.

The first order of phase transition was proved by the temperature hysteresis of about $\delta T \approx 0.5$ K observed in the thermal cycling experiments.

It should be noted that after heating from temperature below T_0, optical homogeneity of the sample at room temperature was broken. In Fig. 3e one can see bright heterogeneous fibers existing for a long time.

In order to see that the ferroelastic phase transition in $(NH_4)_2SnF_6$ is not accompanied by appearance of the ferroelectricity, the behaviour of dielectric properties was also examined. The measurements of permittivity and dielectric losses were performed by means of an E7-20 immitance meter at a frequency of 1 kHz upon heating at a rate of about 0.6 K/min in the

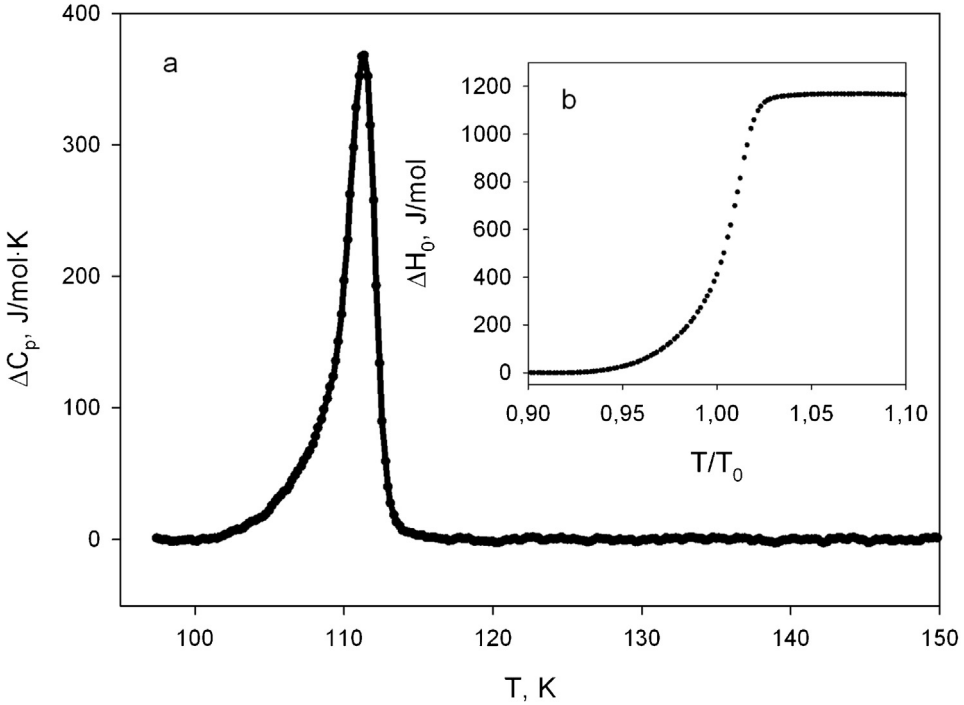

Fig. 2. Temperature dependencies of the excess heat capacity (a) and enthalpy (b) of $(NH_4)_2SnF_6$ extracted from DSM data.

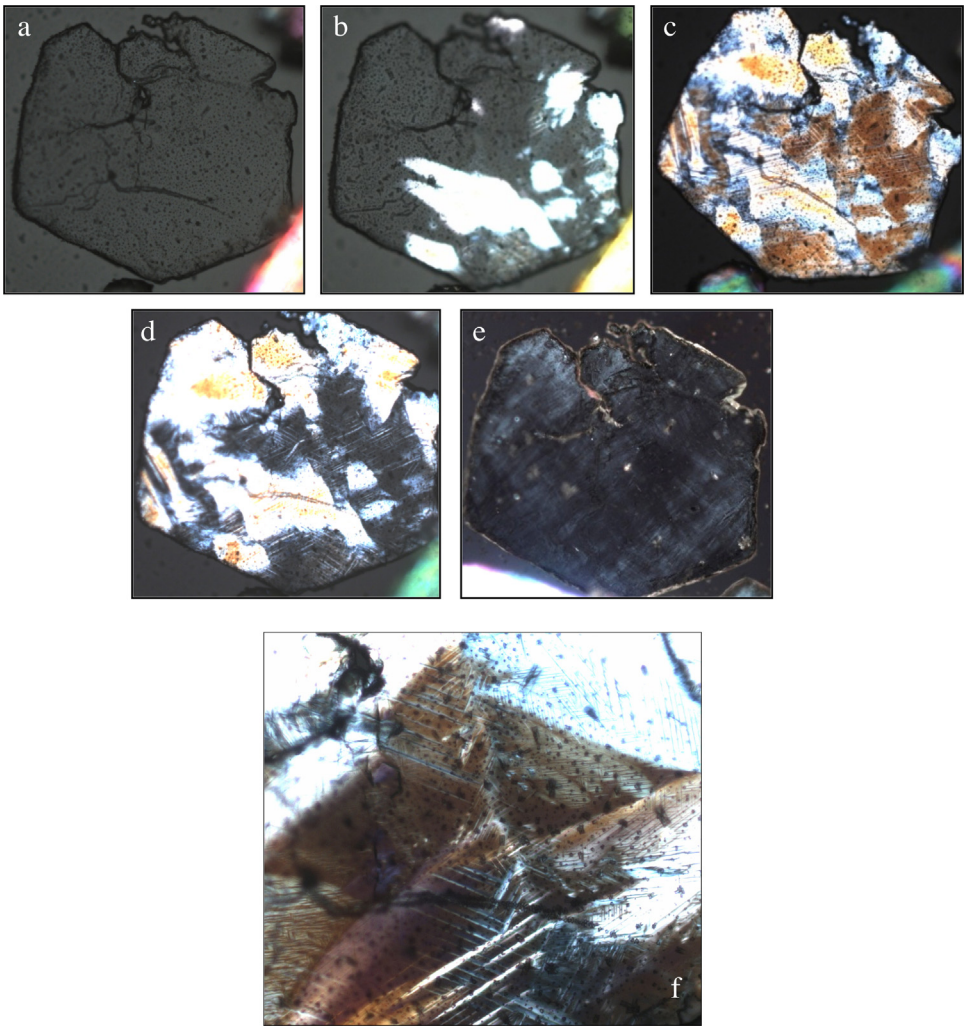

Fig. 3. Observation of the crystal plate (0 0 1) of $(NH_4)_2SnF_6$ in polarized light at $T = 300$ K (a), at $T < 110$ K (appearance of anisotropy (b, c) and the position of extinction (d)), at $T = 300$ K after heating from low temperature phase (e), twin boundaries with high magnification (f).

temperature range 100–300 K. The study of dielectric properties was carried out on the ceramic sample in the form of pressed pellet (8 mm in diameter, 3.5 mm in height) prepared from fine powder without heat treatment. Electrodes were formed by conducting glue covered the opposite flat sides of the sample.

Fig. 4a and b demonstrate the small step-wise anomaly about 2 units at ~110 K of the permittivity and nonanomalous behaviour of $tg\delta(T)$.

Such behaviour of the dielectric properties provides no evidence for the ferroelectric nature of transformation and polar phase in ammonium hexafluorostannate below T_0. A rather strong increase of $\varepsilon(T)$ as well as $tg\delta(T)$ above 270 K is, most likely, connected to the dielectric losses in the ceramic sample prepared without heat treatment.

The results obtained prove the centrosymmetric phase P-1 assumed below T_0 on the ground of optical studies.

Thus, the behaviour of the thermal, optical and dielectric properties revealed the existence of structural transformation in trigonal $(NH_4)_2SnF_6$ at $T_0 = 110$ K, which is ~70 K greater than T_0 in trigonal $(NH_4)_2SiF_6$ [9]. Because the temperature attachment of a Bruker D8 ADVANCE powder diffractometer did not operate below 120 K, we were not able to solve the low temperature structure.

3.2. Heat capacity

In order to obtain information about the behaviour of the molar heat capacity over a wide temperature range and to refine the thermodynamic parameters of the phase transition obtained in DSM measurements, we carried out the experiments on trigonal $(NH_4)_2SnF_6$ by means of a homemade adiabatic calorimeter with three screens [13]. Calorimetric studies were performed in the temperature range 85–270 K on the sample with a mass of 147.6 mg. A reliable thermal contact between the sample and the heater was provided by vacuum grease.

Using the data about the heat capacities of the heater and contact grease determined in separate experiments, information on the heat capacity of the sample was obtained. Calorimetric experiments were performed using both the discrete ($\Delta T = 1.0$–5.0 K) and continuous ($dT/dt = 0.01$–0.30 K/min) heating. The error of heat capacity determination was about 0.2–0.4% in the whole temperature range investigated.

The molar heat capacity data as a function of temperature are plotted in Fig. 5a.

One can see that experiments with the adiabatic calorimeter identify only one anomaly of heat capacity around $T_0 = 110.3 \pm 0.3$ K associated with the phase transition found first of all by DSM.

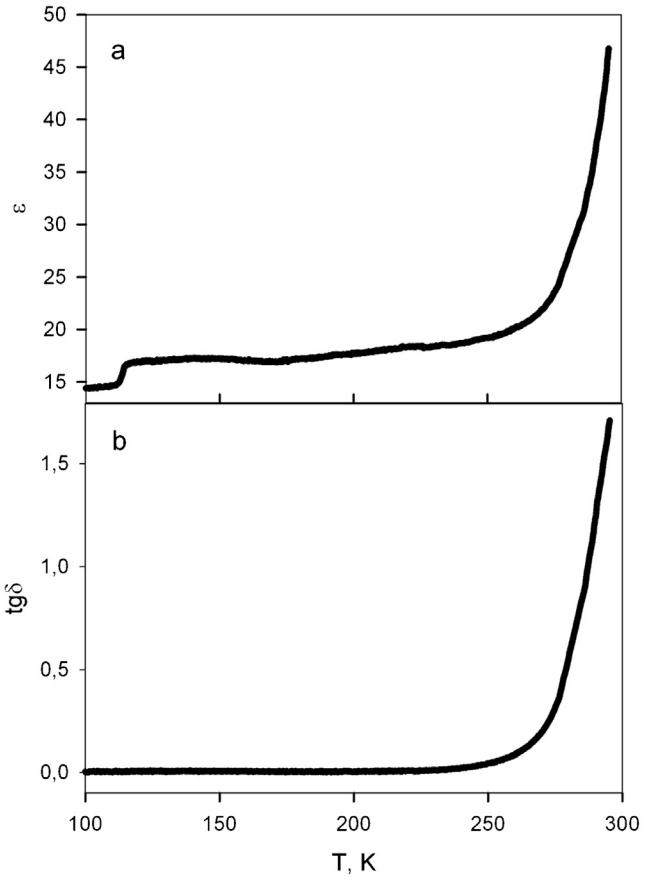

Fig. 4. Temperature dependencies of permittivity (a) and dielectric losses (b) of $(NH_4)_2SnF_6$.

To analyse the thermodynamic parameters of phase transition in greater detail, the anomalous ΔC_p and lattice C_L contributions to the total heat capacity should be separated. This procedure was carried out using a simple model describing the lattice heat capacity of the compound as a combination of the Debye and Einstein functions. In the temperature range 85–270 K, the heat capacity of the sample under investigation is already poorly sensitive to fine details of a vibration spectrum and the approximation of the lattice contribution carried out in this way is quite justified.

The enthalpy change at the phase transition was determined by integration of the $\Delta C_p(T)$ function within the corresponding temperature range $\Delta H_0 = 1800 \pm 110$ J/mol. It is seen that this value is substantially larger than that following from the DSM data. This finding is not surprising, because the sensitivity of scanning calorimeter to heat effects is lower compared to the adiabatic method.

One of the parameters characterising the mechanism of phase transition is the entropy change value, which can be determined integrating the function $(\Delta C_p/T)(T)$. A large value of $\Delta S_0 = 16.4 \pm 1.0$ J/mol K found by this means for $(NH_4)_2SnF_6$ (Fig. 5b) allows one to think that structural transformation P-3m1 ↔ P-1 is associated with some order-disorder processes.

Small thermal parameters of fluorine atoms vibrations found in the present study and in the previous ones for $(NH_4)_2SnF_6$ [6] as well as for $(NH_4)_2SiF_6$ [11] show that octahedral structural units are ordered in P-3m1 phase of both crystals. Thus, the phase transition of order-disorder type may be related to the ordering only NH_4 tetrahedra. For $(NH_4)_2SnF_6$ only one orientation of NH_4 group was conferred at room temperature [6] and tetrahedron seemed to be ordered. But geometry of this tetrahedron was far from ideal and it was suggested that such a model did not correspond to reality. Moreover, the determination of H atoms using X-ray data is a very

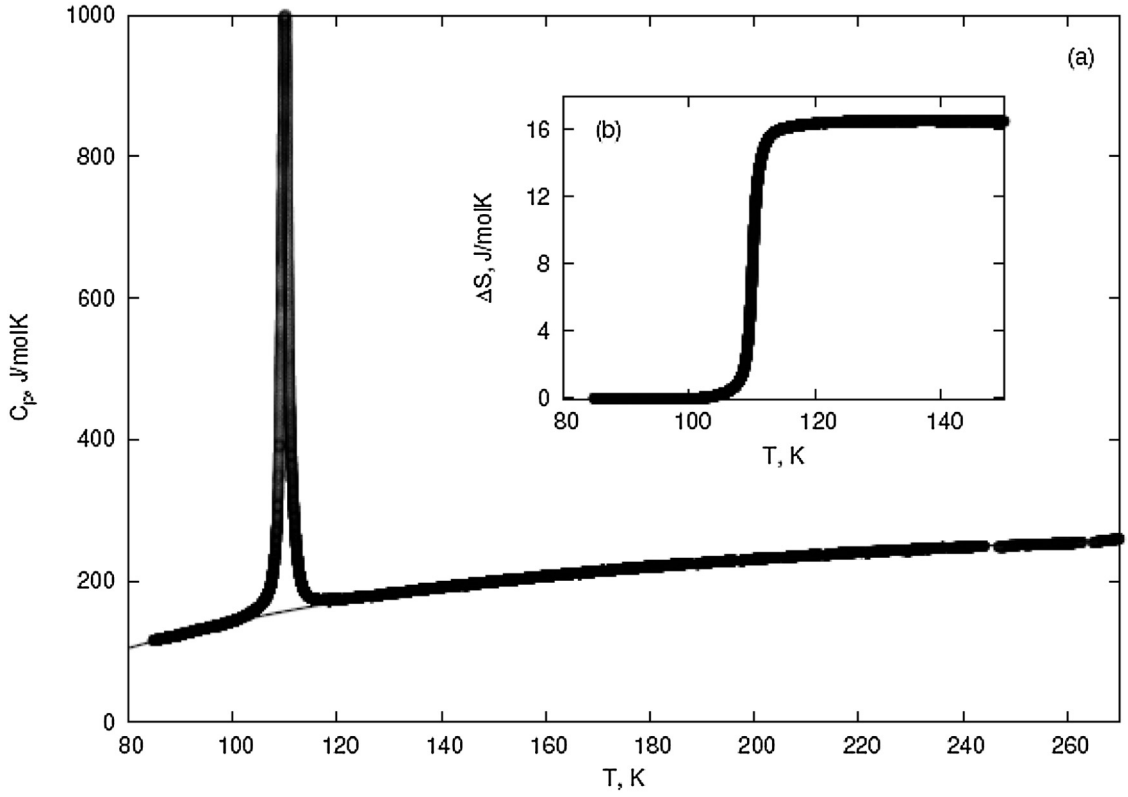

Fig. 5. Temperature dependence of the molar heat capacity of $(NH_4)_2SnF_6$. Dashed line is the lattice heat capacity (a). The excess entropy behaviour is (b).

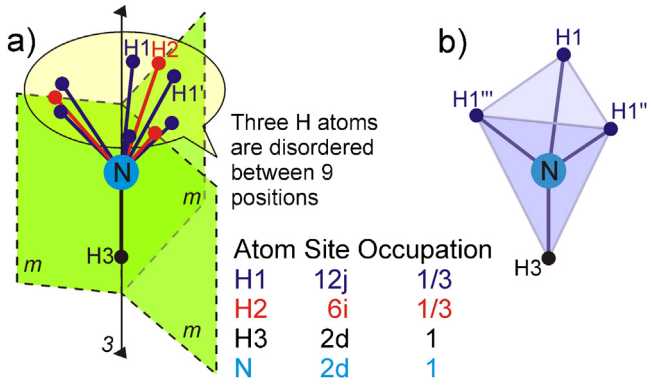

Fig. 6. Scheme of NH_4 tetrahedron: disordering between 3 orientations at room temperature (a); one orientation in the low-temperature phase (b).

complex task due to the low value of atomic function of hydrogen atom, and usually the real positions of H atoms remain unclear.

However, the large value of entropy change and triclinic symmetry of the $(NH_4)_2SnF_6$ low-temperature phase with probable full ordering of all structural units enable us to suggest that NH_4 tetrahedra should be disordered at least on 3 orientations at room temperature. In this case, the previous model [6] should be somewhat corrected. Since the N atom of the tetrahedron is located in the 2d Wyckoff site with local 3 m symmetry, so 3 orientations of NH_4 tetrahedra can be generated using one H atom in general 12j site, one H atom in special 6i site with occupancies of 1/3 (Fig. 6a) and one H atom in special position 2d with occupancy of 1, similarly Ref. [6]. Below the phase transition point, only one orientation of NH_4 remains (Fig. 6b) and the entropy change associated with the ordering of two tetrahedra in the unit cell is equal to $\Delta S_0 = R\ln(N2/N1) = 2R\ln(3/1) = R\ln 9 = 18.3$ J/mol K, which is close to the experimental value 16.4 ± 1.0 J/mol K.

It is necessary to point out that the phase transition entropy found experimentally for $(NH_4)_2SiF_6$ is significantly less, $\Delta S_0 = 5.9$ J/mol K $\approx R\ln 2$ [10]. This ΔS_0 value corresponds to twofold disorder of the NH_4 group suggested [11]. Tetrahedra were assumed to be reflected in a pseudomirror plane perpendicular to the trigonal axis.

It is interesting that neutron and NMR studies have shown that in cubic $(NH_4)_2SiF_6$ the threefold proton disorder in the NH_4 groups is dynamic but not static [14,15]. Thus, one can suppose that total ordering octahedral and tetrahedral structural elements is the reason why cubic modification of hexafluorosilicate does not undergo any structural transformation.

3.3. Thermal expansion

The thermal expansion of $(NH_4)_2SnF_6$ was studied in the temperature range of 100–600 K with a heating rate of 3 K/min by a Netzsch model DIL-402C pushrod dilatometer. The investigations were performed under a helium atmosphere flowing at 40 mL/min. The influence of system thermal expansion was removed by calibration of the results with quartz and Al_2O_3 as standard References

The measurements of linear thermal expansion coefficient $\alpha(T)$ were carried out on a ceramic sample used previously in dielectric studies. One $\alpha(T)$ anomaly associated with phase transition was observed at $T_0 = 113.0 \pm 0.5$ K. This value is slightly higher than those obtained in other experiments, which is a result of the dynamic nature of thermal expansion measurements.

The temperature dependencies of both $\alpha(T)$ and linear strain $\Delta L/L$ in the region of structural transformation are shown in Fig. 7.

One can also see some interesting points. First, the linear thermal expansion coefficient of $(NH_4)_2SnF_6$ is negative between

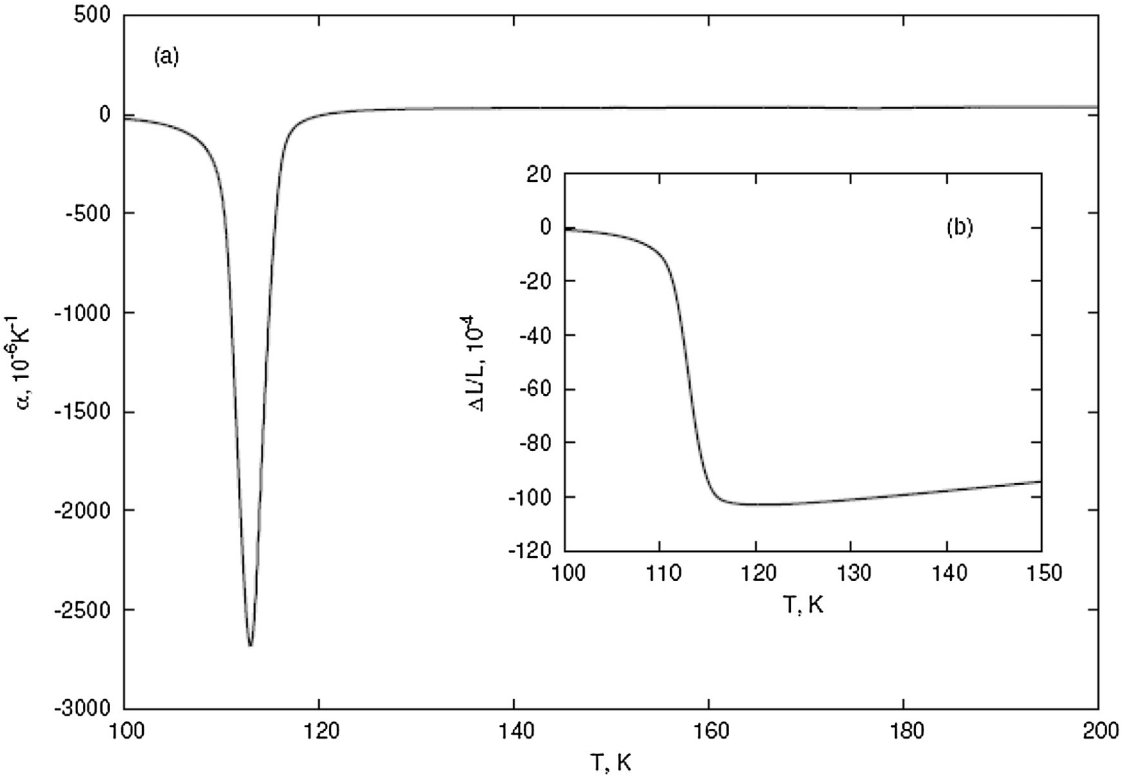

Fig. 7. Temperature dependencies of thermal expansion coefficient (a) and strain (b).

100 and 120 K, which correlates with the decrease of the unit cell volume upon heating from P-1 phase. Secondly, the change of linear size of the sample in the region of structural transformation is very large (~1%).

3.4. Effect of hydrostatic pressure

The susceptibility of $(NH_4)_2SnF_6$ to external pressure was experimentally studied using differential thermal analysis (DTA) allowing to detect the heat capacity anomalies. High sensitive germanium–copper thermocouple was used as a sensor. The powdered sample of 0.05 cm^3 volume was placed in a copper container glued onto one junction of a thermocouple. The quartz sample as a reference substance was cemented to the other junction. The measurements were performed for both increasing and decreasing pressure cycles, to ensure the reliability of the results. The details of the measurement procedure have been described earlier [16].

The results of the experiments with pressure are displayed in Fig. 8.

At ambient pressure, the anomalous behaviour of the DTA signal is observed in the range 105–120 K with the peak maximum at $T_0 = 114 \pm 2$ K, which is in a good agreement with the results of calorimetric and dilatometric experiments taking into account the dynamic procedure of the DTA measurements. Increasing the pressure leads to the decrease of the phase transition point, and the boundary between P-3m1 and P-1 phases can be described adequately as linear with a rather large negative baric coefficient $dT_0/dp = -157 \pm 5$ K/GPa. Fig. 8b shows that DTA anomaly connected to the excess heat capacity ΔC_p is smeared with the pressure increase, but the area under peak associated with the enthalpy value $\Delta H_0 = \int \Delta C_p dT$ seems to be unchanged.

Since $(NH_4)_2SnF_6$ undergoes the first order phase transition, the pressure dependence of T_0 can be also evaluated using the Clausius–Clapeyron equation $dT_0/dp = \delta V_0/\delta S_0$, where δV_0 and δS_0 are the discontinuous volume and entropy changes at the phase transition point, respectively. On the one hand, we were unable to determine exactly the jumps of the elongation and the volume at the transition temperature, because the thermal expansion anomaly near the phase transition temperature was smeared out due to the dynamic nature of thermal expansion measurements. On the other hand, the temperature region of structural transformation in $(NH_4)_2SnF_6$ is rather narrow and one can assume that the difference between the total (ΔV_0, ΔS_0) and discontinuous (δV_0, δS_0) values is small. Indeed, estimation of the pressure derivative of the transition temperature using total changes of ΔV_0 and ΔS_0 gives the value $dT_0/dp = -170 \pm 20$ K/GPa, which is close to baric coefficient determined experimentally. This fact unambiguously shows the reliability of information about thermal properties obtained by three independent experimental methods—dilatometric, calorimetric and DTA under pressure.

It is interesting to compare the susceptibility to hydrostatic pressure of hexafluorostannate under study with that characteristic for some other families of perovskite-like compounds. For example, gigantic values of dT/dp (K/GPa) were found for some fluorides with ReO_3 structure ($CoZrF_6$ $dT/dp = 340$ [17]; $Sc_{1-x}AlF_3$ $dT/dp = 500$ [18]) and chloride perovskites ($RbCaCl_3$ $dT/dp = 134$; $KCaCl_3$ $dT/dp = 196$ [17]). In accordance with [19], large baric coefficients allow us to suppose the strong interaction between the order parameter and the strain in these compounds.

3.5. Barocaloric effect

The barocaloric effect (BCE) in ferroics (viz. ferromagnets, ferroelastics and ferroelectrics) associated with the reversible change of entropy ΔS_{BCE} or temperature ΔT_{AD} with pressure under isothermal or isoentropic (adiabatic) conditions attracts a great deal of interest partially due to the possibility of using materials

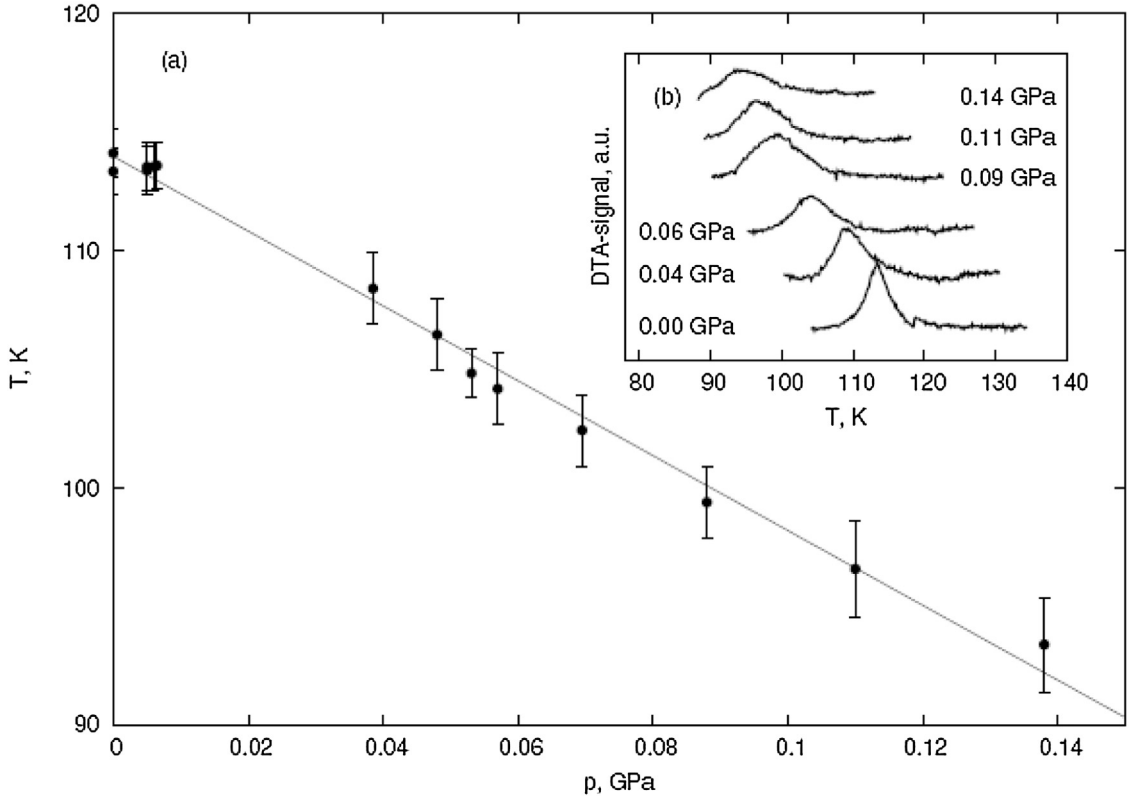

Fig. 8. Temperature–pressure phase diagram (a) and temperature–pressure behaviour of the DTA signal (b).

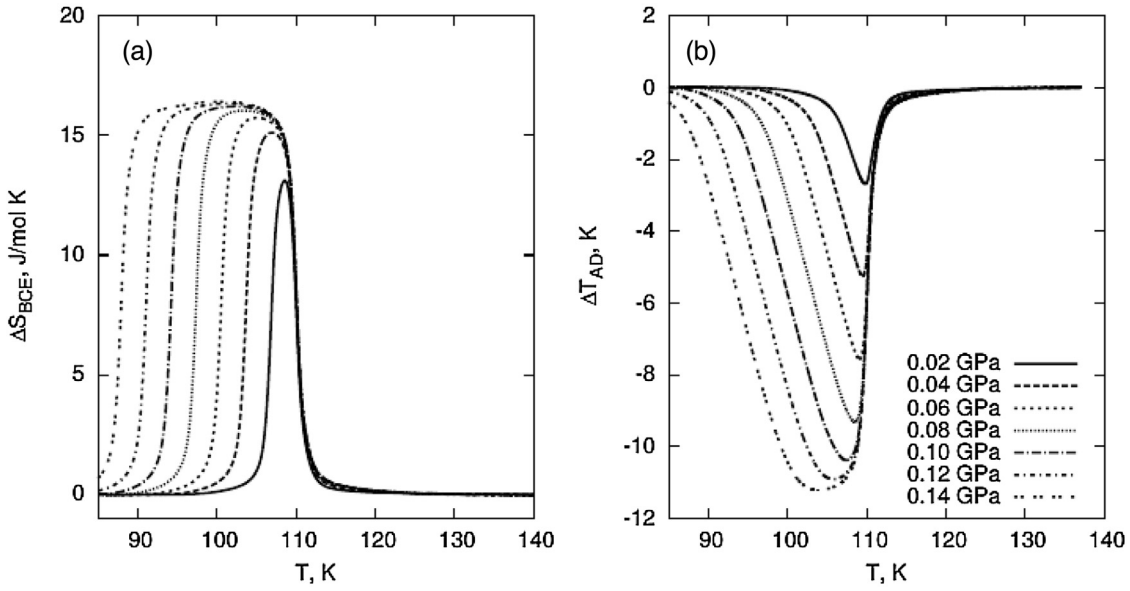

Fig. 9. Temperature dependencies of extensive (a) and intensive (b) BCE in $(NH_4)_2SnF_6$ at pressures in the range from 0 to 0.14 GPa.

with pronounced BCE as solid refrigerants [20–23]. As it has been shown [22,23], ferroics undergoing order–disorder phase transitions associated with large entropy and significant baric coefficient are the most promising compounds for this purpose. In our case, $(NH_4)_2SnF_6$ meets these requirements and we determined the intensive ΔT_{AD} and extensive ΔS_{BCE} BCE by a similar way as it was early done for magnetic, ferroelectric, ferroelastic and martensitic transformations [20–25].

The insignificant change of the phase transition enthalpy $\Delta H_0 = \int \Delta C_p dT$ under pressure (Fig. 8b) means that entropy of transformation is also almost constant. This allows us to assume that in the pressure range investigated, first, there are no significant changes in the proximity of phase transition to the tricritical point and, second, the number of equivalent orientational states of tetrahedral ionic groups in the initial phase is unchanged. A substantial change in regular lattice entropy S_L at low pressure is also most likely absent.

The entropy for $p > 0$ as a function of temperature and pressure was determined by summation of $S_L(T)$ and $\Delta S(T)$, shifted along the temperature scale according to baric coefficient dT_0/dp

$$S(T,p) = S_L(T) + \Delta S[T + (dT_0/dp)\cdot p] \quad (1)$$

Fig. 9 shows the pressure and temperature dependencies of the extensive and intensive BCE determined the following way [22]:

$$\Delta S_{BCE}(T;\ p) = S(T;\ p \neq 0) - S(T;\ p = 0) \quad (2)$$

$$\Delta T_{AD} = -(T/C_p)\cdot \Delta S_{BCE} \quad (3)$$

In accordance with the negative volume change near the phase transition point, BCE in $(NH_4)_2SnF_6$ is inverse, i.e., $\Delta T_{AD} < 0$ and $\Delta S_{BCE} > 0$.

It is obvious that a maximum possible magnitude of the extensive caloric effect is equal to the value of the entropy change associated with phase transition [23]. A very important point is that the maximum value of $\Delta S_{BCE}{}^{MAX} = \Delta S_0 = 16.4$ J/mol K was reached in $(NH_4)_2SnF_6$ at low pressure ~0.1 GPa (Fig. 9a). Somewhat higher pressure (~0.15 GPa) is needed to realise the maximum intensive BCE $\Delta T_{AD}{}^{MAX} \approx 12$ K.

Both extensive and intensive barocaloric parameters of $(NH_4)_2SnF_6$ are comparable to those for materials considered as prominent for use as working bodies in solid refrigeration cycles [21–25]. Indeed, it is seen, for example, from the relationship between specific extensive BCE (J/kg K) determined at rather low pressure: $(NH_4)_2SnF_6$ (ΔS_{BCE} = +61 at 0.1 GPa), Rb_2KFeF_6 (−42 at 0.15 GPa) and $(NH_4)_3MoO_3F_3$ (−55 at 0.07 GPa) [22], Ni–Mn–In alloy (−20 at 0.14 GPa) [25].

4. Conclusions

Calorimetric, dilatometric, optic, dielectric and X-ray studies have revealed that $(NH_4)_2SnF_6$ undergoes first order structural phase transition P-3m1 ↔ P-1 of nonferroelectric nature at about 110 K.

The large changes of entropy ($\Delta S_0 = 16.4$ J/mol K) and volume ($\Delta V_0/V \approx 1\%$) at the phase transition temperature point to the fact that structural distortions can be associated with the ordering of some structural units.

An analysis of X-ray data and optical twinning in the low-temperature phase allowed us to suggest a model of structural disorder in P-3m1 phase associated with 3 possible orientations of NH_4 tetrahedra, which gives the entropy change $\Delta S_0 = R\ln 9 = 18.3$ J/mol K close to the experimental value.

A very high sensitivity of $(NH_4)_2SnF_6$ to hydrostatic pressure is characterised by gigantic baric coefficient $dT_0/dp = -157$ K/GPa, which agrees well with the value estimated from the Clausius–Clapeyron equation (i.e. −170 K/GPa).

An analysis of the entropy against temperature and pressure dependencies showed that the magnitudes of the extensive and intensive barocaloric effects in $(NH_4)_2SnF_6$ are rather large and comparable to the parameters of solid state coolants. The very important point is that the maximum values of ΔS_{BCE} and ΔT_{AD} can be reached in hexaflurostannate at low pressure.

New important information obtained here on the physical properties of fluoride $(NH_4)_2SnF_6$ known for a long time will be useful in developing investigations of related compounds and particularly on the way of searching for effective solid refrigerants.

Acknowledgements

The reported study was partially supported by RFBR, research project No. 15-02-02009a.

References

[1] M. Molokeev, S.V. Misjul, I.N. Flerov, N.M. Laptash, Reconstructive phase transition in $(NH_4)_3TiF_7$ accompanied by the ordering of TiF_6 octahedra, Acta Cryst. B70 (2014) 924–931.

[2] I.N. Flerov, M.S. Molokeev, N.M. Laptash, A.A. Udovenko, E.I. Pogoreltsev, S.V. Mel'nikova, S.V. Misyul, Structural transformation between two cubic phases of $(NH_4)_3SnF_7$, J. Fluorine Chem. 178 (2015) 86–92.

[3] E.I. Pogoreltsev, I.N. Flerov, A.V. Kartashev, E.V. Bogdanov, N.M. Laptash, Heat capacity entropy, dielectric properties and T-p phase diagram of $(NH_4)_3TiF_7$, J. Fluorine Chem. 168 (2014) 247–250.

[4] M.C. Marignac, Recherches sur les formes crystallines et la composition chimique de divers sels, Ann. Min. 15 (1859) 221–290.

[5] R.L. Davidovich, T.A. Kaidalova, Ammonium hexafluorostannate and hexafluoroplumbate, Russ. J. Inorg. Chem. 16 (1971) 1354–1356.

[6] G. Meyer, N. Böhmer, Refinement of the crystal structure of diammonium hexafluorostannate (IV), $(NH_4)_2SnF_6$, Z. Kristallographie 216 (2001) 20.

[7] A. Lari-Lavassani, G. Jourdan, Ch. Avinens, L. Cot, Etude cristallographique d'hexafluorostannates cubicues et hexagonaux $M^1{}_2SnF_6$, C.R. Acad. Sc. Paris 279 (Serie C) (1974) 193–195.

[8] M.C. Marignac, Recherches sur les formes crystallines et la composition chimique de divers sels, Ann. Min. 12 (1857) 1–74.

[9] M.C. Marignac, Recherches chimiques et crystallographiques sur les fluorozirconates, Ann. Chim. Phys. 60 (1860) 257–307.

[10] C.C. Stephenson, C.A. Wulff, O.R. Lundell, Heat capacities of cubic and hexagonal ammonium hexafluosilicate from 25° to 300 K, J. Chem. Phys. 40 (1964) 967–974.

[11] E.O. Schlemper, W.C. Hamilton, On the Structure of Trigonal Ammonium Fluorosilicate, J. Chem. Phys. 45 (1966) 408–409.

[12] Bruker AXS TOPAS V4, General profile and structure analysis software for powder diffraction data. –User's Manual, Bruker AXS, Karlsruhe, Germany. (2008).

[13] A.V. Kartashev, I.N. Flerov, N.V. Volkov, K.A. Sablina, Adiabatic calorimetric study of the intense magnetocaloric effect and the heat capacity of $(La_{0.4}Eu_{0.6})_{0.7}Pb_{0.3}MnO_3$, Phys. Solid State 50 (2008) 2115–2120.

[14] E.O. Schlemper, W.C. Hamilton, J.J. Rush, Structure of cubic ammonium fluosilicate: neutron-diffraction and neutron-inelastic-scattering studies, J. Chem. Phys. 44 (6) (1966) 2499–2505.

[15] R. Blinc, G. Lahajnar, Magnetic resonance study of molecular motion in cubic $(NH_4)_2SiF_6$, J. Chem. Phys. 47 (1967) 4146–4152.

[16] M.V. Gorev, I.N. Flerov, Pressure–temperature phase diagrams of elpasolites Cs_2RbDyF_6 and $Cs_2NaTmBr_6$, Sov. Phys. Solid State 34 (1992) 1401–1403.

[17] I.N. Flerov, M.V. Gorev, K.S. Aleksandrov, Hydrostatic pressure influence on phase transitions in perovskite-like ferroeleastics, Sov. Phys. Solid State 35 (1993) 1657–1666.

[18] C.R. Morelock, L.C. Gallington, A.P. Wilkinson, Solid solubility phase transitions, thermal expansion, and compressibility in $Sc_{1-x}Al_xF_3$, J. Solid State Chem. 222 (2015) 96–102.

[19] I.N. Flerov, M.V. Gorev, K.S. Aleksandrov, Effect of hydrostatic pressure on phase transitions in perovskite-like ferroeleastics, Ferroelectrics 169 (1995) 199–205.

[20] T. Strässle, A. Furrer, Z. Hossain, Ch. Geibel, Magnetic cooling by the application of external pressure in rare-earth compounds, Phys. Rev. B67 (2003) 054407.

[21] P.O. Castillo-Villa, D.E. Soto-Parra, J.A. Matutes-Aquino, R.A. Ochoa-Gamboa, A. Planes, L. Mánosa, D. González-Alonso, M. Stipcich, R. Romero, D. Ríos-Jara, H. Flores-Zúñiga, Caloric effects induced by magnetic and mechanical fields in a $Ni_{50}Mn_{25-x}Ga_{25}Co_x$ magnetic shape memory alloy, Phys. Rev. B83 (2011) 174109 1–6.

[22] I.N. Flerov, M.V. Gorev, A. Tressaud, N.M. Laptash, Perovskite-like fluorides and oxyfluorides: phase transitions and caloric effects, Crystallogr. Rep. 56 (2011) 9–17.

[23] I.N. Flerov, E.A. Mikhaleva, M.V. Gorev, A.V. Kartashev, Caloric and multicaloric effects in oxygen ferroics and multiferroics, Phys. Solid State 57 (2015) 429–441.

[24] E.A. Mikhaleva, I.N. Flerov, V.S. Bondarev, M.V. Gorev, A.D. Vasiliev, T.N. Davydova, Phase transitions and caloric effects in ferroelectric solid solutions of ammonium and rubidium hydrosulfates, Phys. Solid State 53 (2011) 510–517.

[25] L. Mañosa, D. González-Alonso, A. Planes, E. Bonnot, M. Barrio, J.-L. Tamarit, S. Aksoy, M. Acet, Giant solid-state barocaloric effect in the Ni–Mn–In magnetic shape-memory alloy, Nat. Mater. 9 (2010) 478–481.